

Hydrothermal Synthesis of Porous NiO Nanosheets and Application as Anode Material For Lithium Ion Batteries

Yu Yao, Jingjing Zhang, Zhen Wei, Aishui Yu*

Department of Chemistry, Shanghai Key Laboratory of Molecular Catalysis and Innovative Materials, Institute of New Energy, Fudan University, Shanghai 200438, China

*E-mail: asyu@fudan.edu.cn

Received: 29 November 2011 / *Accepted:* 15 January 2012 / *Published:* 1 February 2012

Porous NiO nanosheets prepared by hydrothermal method were tested as anode materials for lithium ion batteries. Scanning electron microscopy (SEM) images showed that the thickness of the sheet is about 100 nm with nanopores on the planes, forming a two-dimensional network structure. The electrochemical measurement showed that the porous NiO nanosheets had better electrochemical performance than bulk NiO. The improvement of the electrochemical properties could be attributed to its unique two-dimensional network structure.

Keywords: NiO, Porous nanosheet, Anode, Lithium ion battery

1. INTRODUCTION

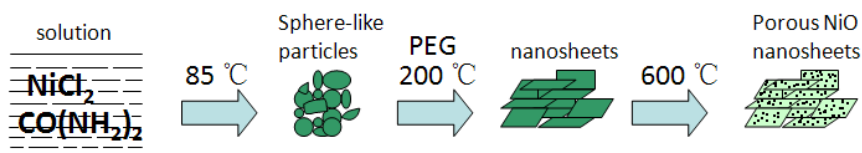
Carbon-based materials are the accepted anode used in the majority of commercial lithium-ion batteries, however, its low capacity cannot meet the increasing energy demand of modern devices. Transition-metal oxides such as Co_3O_4 , NiO, Cu_2O , CuO, Fe_2O_3 , and SnO_2 with higher specific capacity [1-6], have attracted much attention recently [7-9]. Different from the mechanism of lithium insertion/deinsertion in carbonaceous compounds, the metal oxide particles are disintegrated into metallic nanoparticles and Li_2O matrix during the discharge and converted back to metal oxide nanograins during the subsequent charge. However, the capacities of unmodified materials often fade very quickly during charge-discharge cycling. There are many ways to overcome this drawback. Preparation of composite with carbon is a common method, but this method often reduces mass specific capacity. To improve the cyclability without capacity loss, lots of research work was focused on preparing materials with special morphology to enhance the electrochemical performance. Up to date Various structure materials have been prepared, such as nanotubes[10,11], nanoarrays[12,13], microshperes[14-16]. These structures can improve electrochemical performance mainly due to their

large specific surface area, short diffusion length of lithium ions, and good ability of buffering the volume change during electrochemical reaction. Among the transition-metal oxides, NiO has the theoretic capacity of 718 mAh g^{-1} which is higher than CuO and Cu_2O , and it is less expensive than CoO[17] which means that it could be a promising material as anode for lithium ion batteries. Recent years lots of works for NiO have been done, and various special structure materials were reported. L Yuan prepared Spherical Clusters of NiO Nanoshafts[15], S.A. Needham et al. synthesized NiO nanotubes[18], Liu et al. prepared nanosheets-based NiO microspheres[19] and hollow NiO microspheres had been produced by XH Huang et al. [20]. These materials showed good electrochemical performance because of their special structure.

In this work, we proposed a novel approach to prepare unique porous NiO nanosheets. The synthesis involved first forming precursor by a chemical bath deposition method, and then obtaining nanosheets from a hydrothermal method with heat treatment. The electrochemical properties of the nanosheets were investigated by galvanostatic discharge-charge test and cyclic voltammetric analysis (CV).

2. EXPERIMENTAL

2.1. Preparation of porous NiO nanosheets



Scheme 1. Illustration for the synthetic procedure of porous NiO nanosheets

The synthetic procedure is described in Scheme 1. In a typical synthesis, 0.68 g $\text{NiCl}_2 \cdot 6\text{H}_2\text{O}$, 0.96 g urea and 0.4 g PEG-2000 were dissolved in 40 ml deionized water. The solution was then put into a 50 ml Teflon-lined stainless steel autoclave and remained at 85 °C for 24 h. Urea is a widely used agent for homogenous precipitation or homogenous film growth. It acts as a slow-released PH adjusting agent and provides carbonate, so the obtained precursor was a kind of nickel carbonate. The autoclave continued to heat to 200 °C and kept for 24 h. After cooling down to room temperature, a green precipitate was collected and washed several times with deionized water. This precipitate was dried at 70 °C, and subsequently annealed at 600 °C in a Muffle furnace for 3 h. When cooled to room temperature, the porous NiO nanosheets were obtained. The precursor obtained at 85 °C was also calcined to 600 °C for 3 h to form bulk NiO.

2.2. Characterization

The morphology of as-prepared porous NiO nanosheets was observed by scanning electron microscopy (SEM, JEOL JSM-6390). X-ray diffraction (XRD) pattern was performed on a Brüker D8

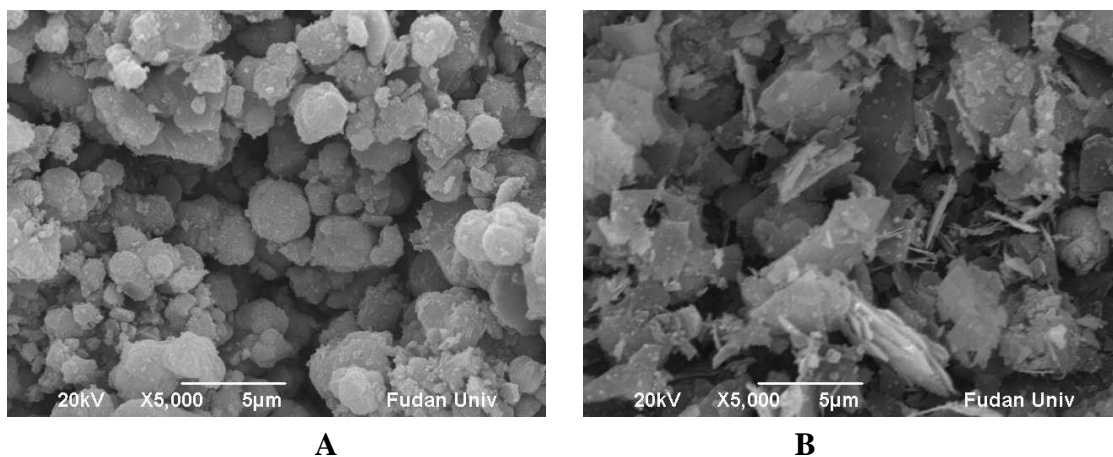
Advance and Davinci Design X-ray diffractometer using Cu K α radiation with a λ of 1.5406 Å at a scan rate of 4° min⁻¹ from 10 to 90°.

2.3. Electrochemical measurement

The electrochemical performance of the as-prepared porous NiO nanosheets materials was evaluated using coin cells assembled in an argon-filled glove box (Mikarouna, Superstar 1220/750/900). An assembled coin cell was composed of lithium as the counter electrode and the working electrode prepared by active materials, super P carbon black and polyvinylidene fluoride (PVDF) with a weight ratio of 80:10:10, using 1-methyl-2-pyrrolidinone (NMP) as the solvent onto a copper foil. The resulting film was dried at 80 °C in vacuum for 12 h in order to evaporate the NMP. 1M LiPF₆ was dissolved in a mixed solvent of ethylene carbonate (EC) and dimethyl carbonate (DEC) (1:1 in volume) to act as the electrolyte and microporous polypropylene film (Celgard 2300) was used as separator. The electrochemical performance of the as-prepared materials was tested by cyclic voltammetry, galvanostatically charging and discharging tests. Cyclic voltammetry was carried out in the potential range from 3 V to 0 V (vs. Li/Li⁺), at a scan rate of 0.2 mV s⁻¹ on an electrochemical workstation (CH Instrument 660C, CHI Company). The galvanostatic charge –discharge tests were performed on a battery test system (Land CT2001A, Wuhan Jinnuo Electronic Co. Ltd) at a current density range of 100-600 mA g⁻¹ within the potential range from 0.01 to 3.0 V. EIS measurements were measured for the fresh cells at open potential with an ac amplitude of 5 mV over the frequency range from 100k to 0.01 Hz.

3. RESULT AND DISCUSSION

Fig.1 (a, b, c, d) display SEM images of the precursor obtained at 85 °C, 200 °C, the porous NiO nanosheets and bulk NiO respectively, their magnified images are exhibit as Fig.1 (e, f, g, h). From Fig.1 (e) we can see sphere-like particles with an average diameter of 1-4 μm, they were deposited during decomposing of urea at 85 °C.



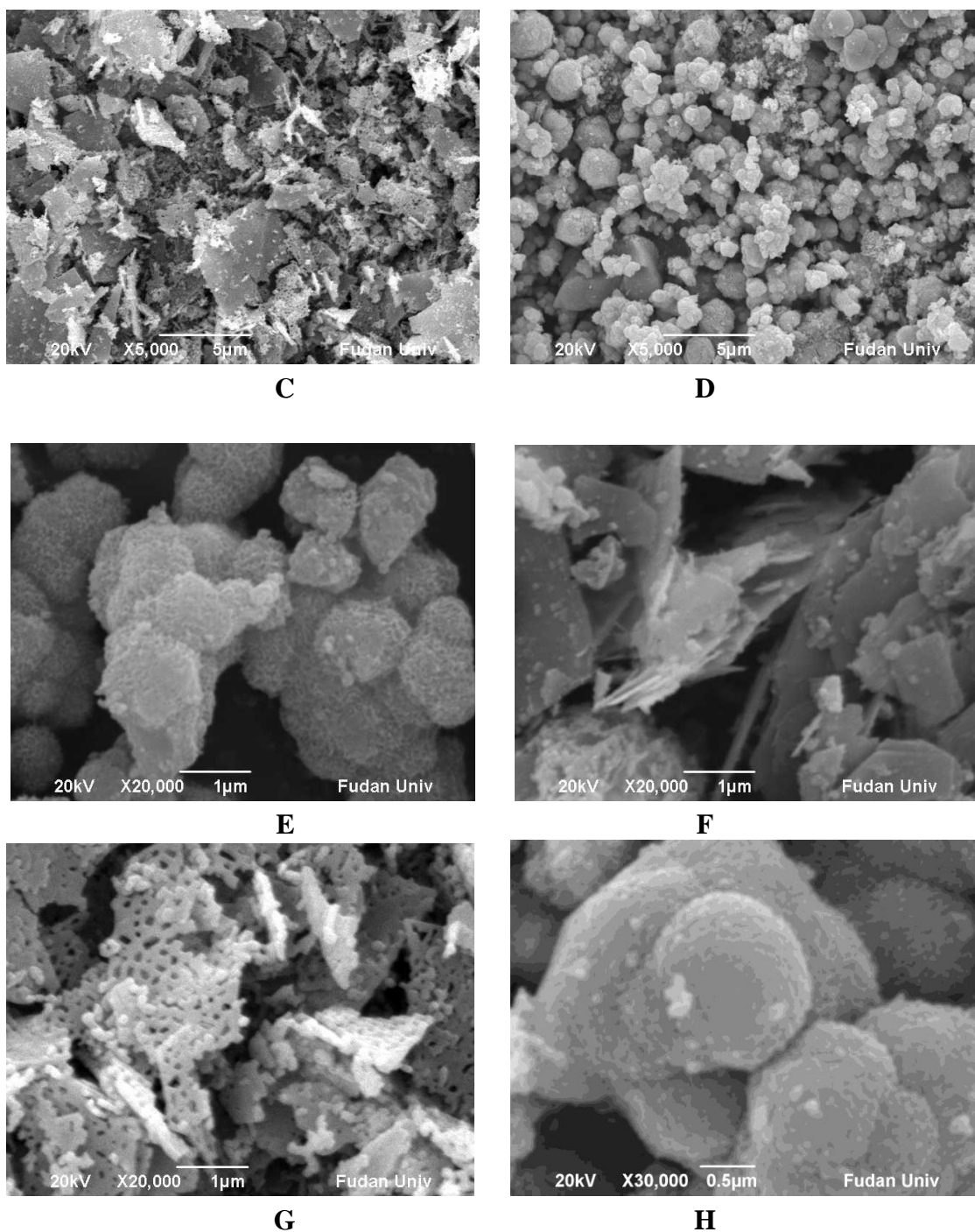


Figure 1. SEM images of the precursor obtained at 85 °C (a and e), the sheets synthesized at 200 °C (b and f), porous NiO sheets (c and g) and bulk NiO (d and h).

Fig.1 (f) displays the image of nanosheets which were formed at 200 °C with assistance of PEG. These nanosheets were change from the sphere-like particles as shown in Fig.1 (e). PEG with uniform and ordered chain structure is easily adsorbed at the surface of metal oxide colloid. When the surface of the colloid adsorbs PEG molecular, the growth rate of the colloids in some certain direction will be confirmed, which finally leads to anisotropic growth of the crystals. So with the existence of PEG, the hydrothermal product presented a shape of sheet. Fig.1 (g) shows the magnified image of the

nanosheets after being calcined to 600 °C, it is clear that the porous nanosheets are about 100 nm in thickness, and a few microns in the length and width. There were many nanopores spreading on the sheets, forming a two-dimensional network. However, the nanosheets without heat treatment had a smooth surface. So the nanopores might be generated by the decomposing of the precursor and the release of water and carbon dioxide. Fig.1 (h) shows the bulk NiO changed from the precursor obtained at 85 °C, and the morphology of bulk NiO was slightly different from the original precursor.

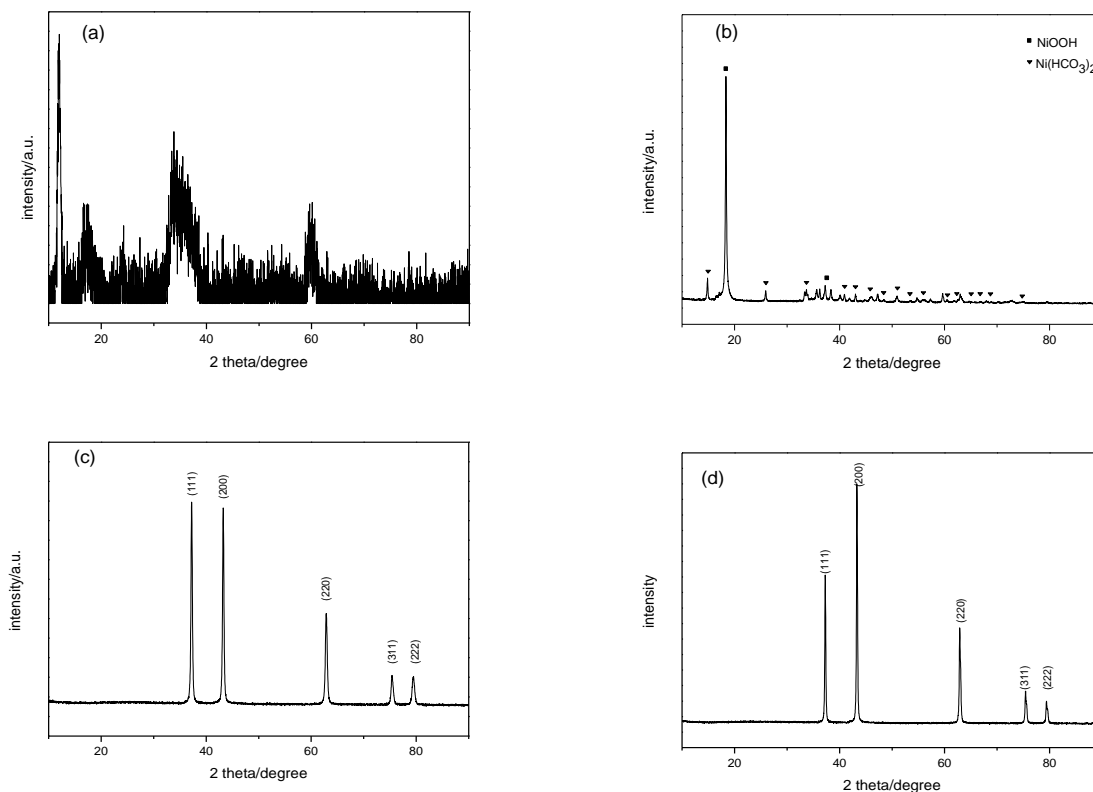


Figure 2. XRD pattern of the precursor obtained at 85 °C (a), the sheets formed at 200 °C (b), porous NiO nanosheets (c) and bulk NiO (d).

The crystal structures of porous NiO nanosheets and their precursor were characterized by XRD. Fig.2a shows the XRD pattern of the precursor obtained at 85 °C and no obvious diffraction peak is found, indicating that the precursor is amorphous. After hydrothermal treatment at 200 °C for 24 h, the product exhibits diffraction peaks which can correspond to NiOOH (JCPDS, No. 06-0141) and Ni(HCO₃)₂ (JCPDS, No. 15-0782) as shown in Fig.2b. Fig.2c displays the XRD pattern of porous NiO nanosheets and bulk NiO. The peaks at 37.1°, 43.1°, 62.6°, 75.0°, and 79.0° can be assigned to the (111), (200), (220), (311), and (222) reflections of NiO respectively. The diffraction pattern corresponds well with the cubic NiO (JCPDS, No. 71-1179), and no diffraction peaks of other impurities are detected. The crystallite size of the porous NiO nanosheets is estimated by the Scherrer equation and the average size of the crystallite is calculated to be about 26 nm. Fig.2d shows the XRD pattern of bulk NiO, its crystallite size is also be estimated. The average crystallite size of bulk NiO is

calculated to be about 37 nm, which is bigger than that of porous NiO nanosheets. It shows the porous NiO sheets are composed by smaller crystallites.

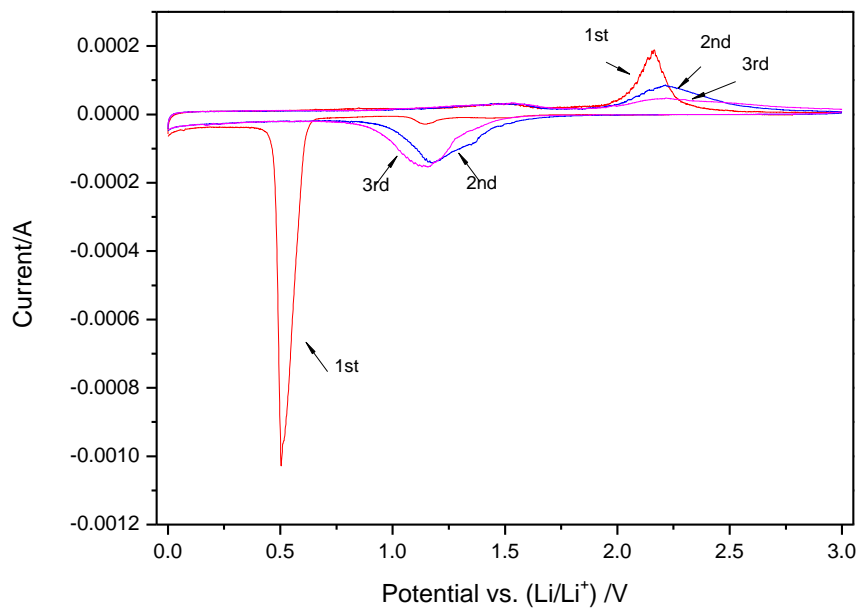


Figure 3. Cyclic Voltammograms of porous NiO nanosheets electrode measured between 0 and 3V at the scan rate of 0.2 mV s^{-1} .

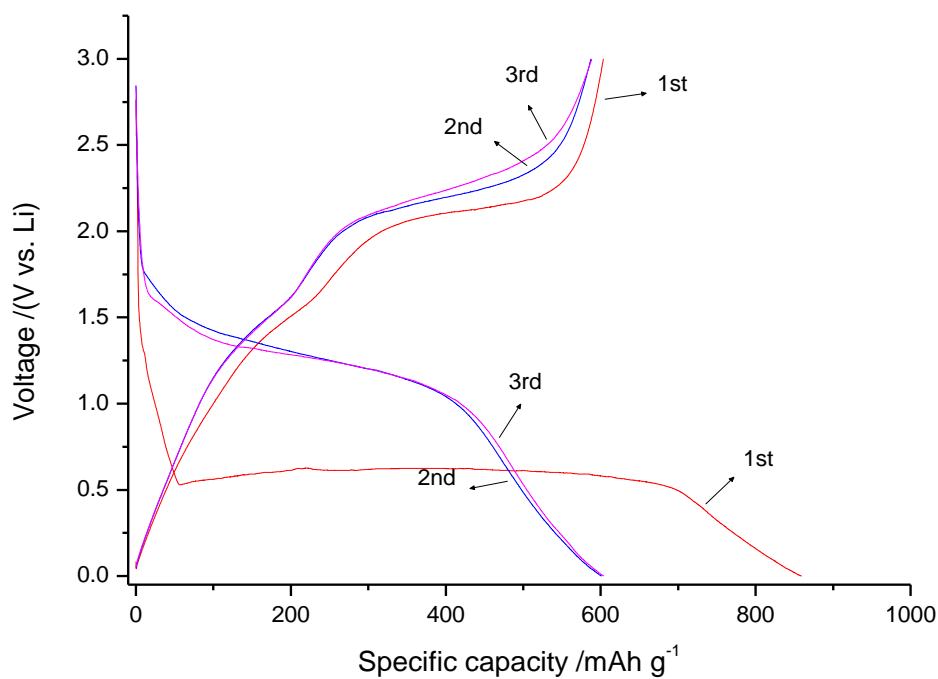
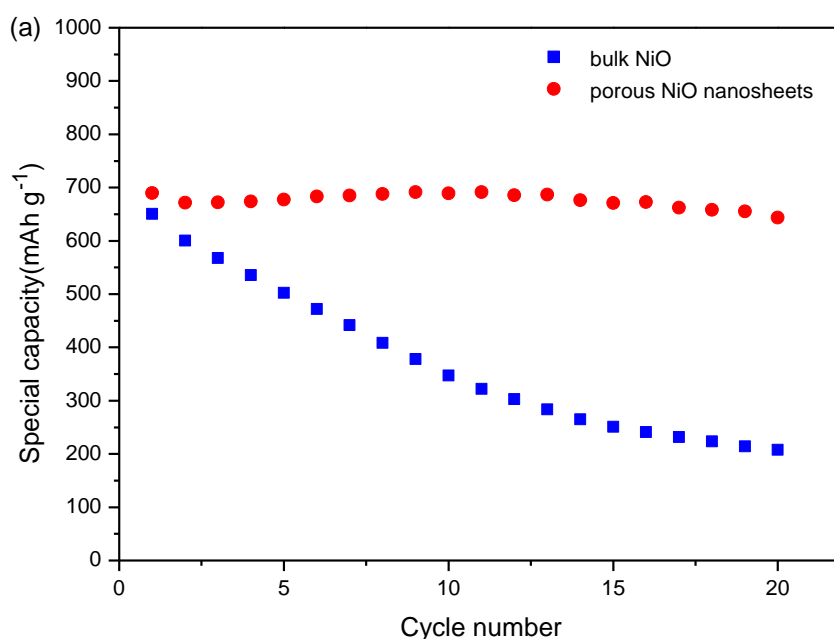


Figure 4. The first three discharge and charge curves of the porous NiO nanosheets at a current density of 100 mA g^{-1} . Inset is the cycling performance.

Cyclic voltammetry measurements were performed to test the electrochemical properties of the porous nanosheets. Fig.3. exhibits the first three complete cycles performed at a sweep rate of 0.2 mV s^{-1} from 0 to 3 V. In the first reduction process, a strong reduction peak at 0.5 V is observed, corresponding to the initial reduction of NiO to metallic Ni ($\text{NiO} + 2\text{Li} \rightarrow \text{Ni} + \text{Li}_2\text{O}$) and the growth of the gel-like solid electrolyte interphase (SEI) layer which contains ethylene-oxide-based oligomers, LiF, Li_2CO_3 , and lithium alkyl carbonate (ROCO_2Li)[8]. In the first oxidation process, there are two peaks at 1.5 V and 2.2 V. The peak at 1.5 V is weak and corresponds to the dissolution of the SEI layer. The peak at 2.2 V is strong and corresponds to the reaction $\text{Ni} + \text{Li}_2\text{O} \rightarrow \text{NiO} + 2\text{Li}$. In the subsequent second and third cycles, the reduction peak shift to 1.2 V and becomes weaker.

Fig.4. presents the discharge and charge curves for the first three cycles of the porous NiO nanosheets in the range of 0.01 to 3 V at a current density of 100 mA g^{-1} . In the first discharge process, the potential drops rapidly to a long flat plateau at about 0.5 V, which corresponds to the reaction $\text{NiO} + 2\text{Li} \rightarrow \text{Ni} + \text{Li}_2\text{O}$. The plateau is followed by a gradual curve decrease from 0.5 to 0 V which corresponds to the formation of the SEI layer. The first discharge capacity delivered 977 mAh g^{-1} , higher than the theoretical capacity (718 mAh g^{-1}). It is possible that the extra capacity comes from the formation of gel-like SEI layer on the surface of the sheets during the first discharge. In the 2nd and 3rd discharge curve the plateaus are not obvious and move to about 1.25 V. The first charge capacity is 689 mAh g^{-1} . In the first charge, there is a plateau at about 2.2 V which corresponds the reaction $\text{Ni} + \text{Li}_2\text{O} \rightarrow \text{NiO} + 2\text{Li}$. In the sequent charges process, the plateau disappears gradually. The potential hysteresis becomes small which indicates that the reaction becomes more reversible since the second cycle.

The charge capacities of the porous NiO nanosheets and bulk NiO for each cycle at the current density of 100 mA g^{-1} are plotted in Fig.5(a).



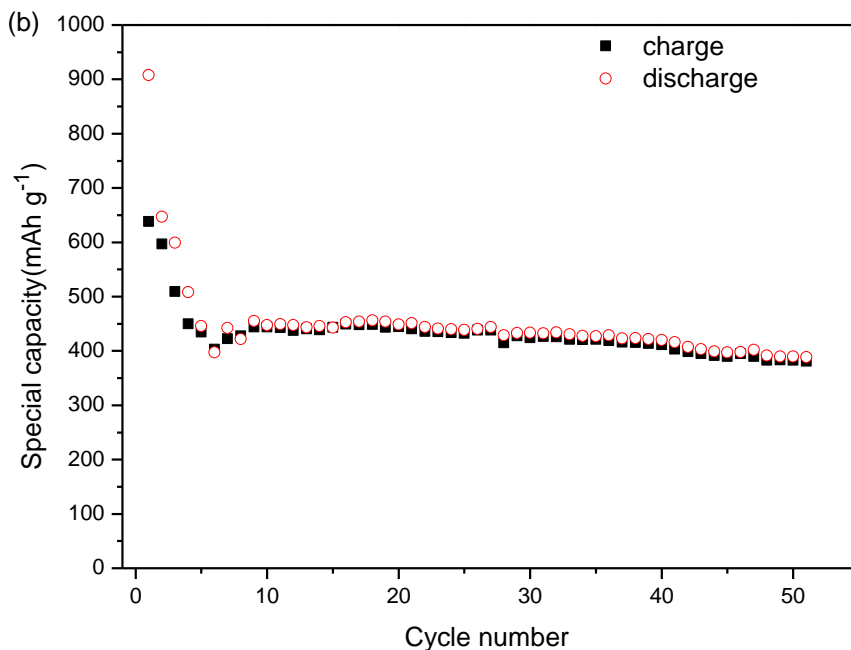


Figure 5. (a) Cycling performance of porous NiO nanosheets and bulk NiO at the current density of 100 mA g⁻¹ (b) cycling performance of porous NiO nanosheets at the current density of 400 mA g⁻¹.

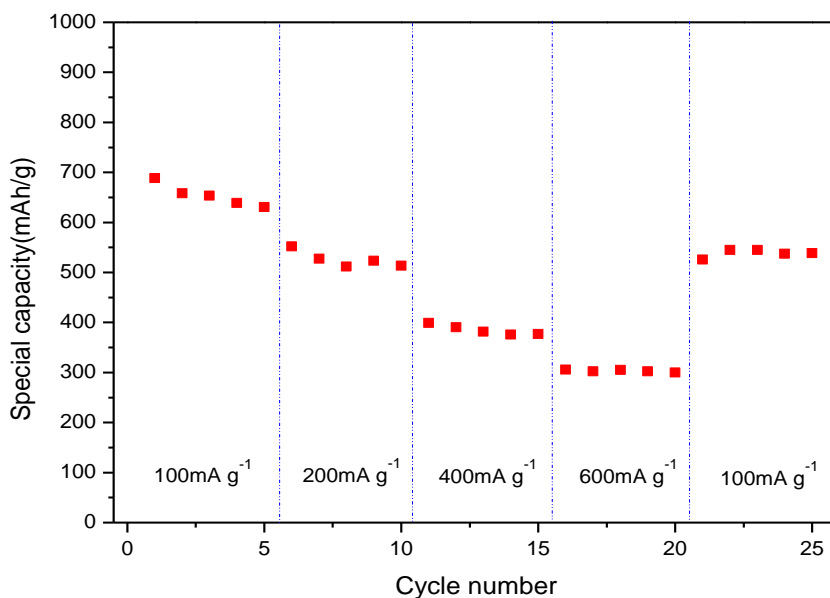


Figure 6. The electrochemical performance of porous NiO nanosheets by multiple step galvanostatic testing (at current density of 100, 200, 400, 600 mA g⁻¹ and then return to the 100 mA g⁻¹ step by step).

The charge capacity of bulk NiO drop quickly and it remains 208 mAh g⁻¹ after 20 cycles. In th contrast, the charge capacity of porous NiO nanosheets decreased very slowly, and the reversible

capacity remains 644 mAh g^{-1} after 20 cycles. However, in the recent study on the Spherical Clusters of NiO Nanosheets[15] and hollow NiO microspheres [20], the 20th cycle capacity of these material is below 600 mAh g^{-1} at the same current density. Fig.5(b) shows cycling performance of porous NiO nanosheets at the current density of 400 mA g^{-1} . It displays that the capacities drop quickly in the first 5 cycles, and then maintain at about 400 mAh g^{-1} up to 50 cycles. The high rate electrochemical performance of porous NiO nanosheets was also investigated by multiple-step galvanostatic strategy and the results are shown in Fig.6. For each step, 5 cycle were measured to evaluate the rate performance. The discharge capacities of porous NiO nanosheets at 100, 200, 400 and 600 mA g^{-1} were 689, 552, 399 and 306 mAh g^{-1} , respectively, much higher than that of commercial graphite. The good electrochemical performance of the porous NiO nanosheets can be attributed to its special nanostructure. The pores on the thin sheets form a net-like structure which let electrolyte easily fill in, leading to large contact interfaces between electrode and electrolyte and short diffusion paths for lithium ions. The porous structure can also accommodate the volume change to alleviate the pulverization. These aspects lead to the improvements of the electrochemical properties.

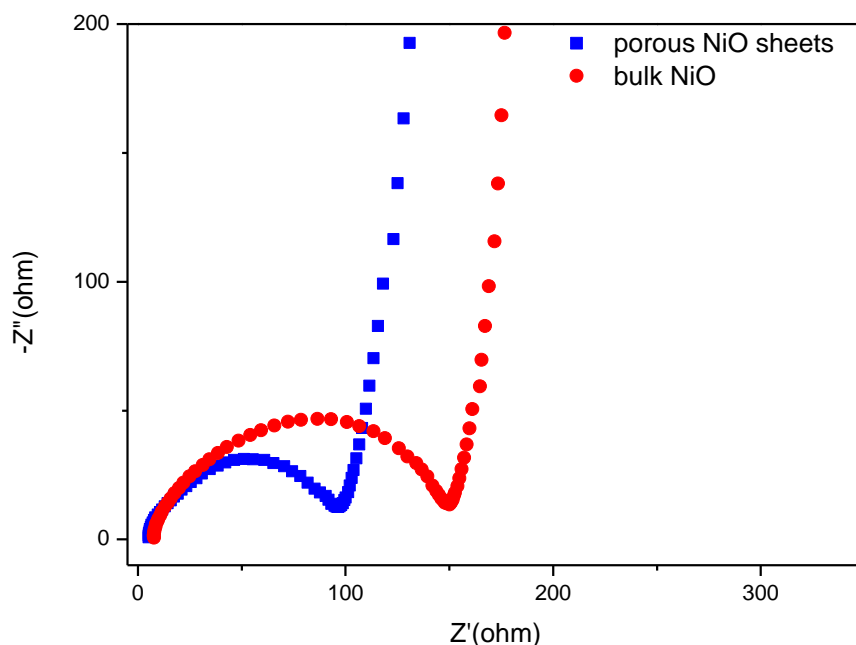


Figure 7. Electrochemical impedance spectra of porous NiO sheets and bulk NiO.

Impedance experiments were applied to explore the effect of porous nanosheets structure on the interfacial impedance of NiO materials. Fig.7 shows the electrochemical impedance spectrum (EIS) of the porous NiO sheets and bulk NiO. The semicircle is attributed to SEI film resistance and the charge-transfer impedance on electrode/electrolyte interface. The inclined line corresponds to the lithium diffusion process within electrodes. It is obviously shown that the diameter of the semicircle for the porous NiO sheets electrode is smaller than that of bulk NiO, indicating lower interfacial impedances. It means that porous NiO nanosheets present better electric contact with electrolyte than bulk NiO.

4. CONCLUSIONS

We developed a novel approach to prepare porous NiO nanosheets for lithium ion battery applications. The thickness of these nanosheets was about 100 nm and there were nanopores on the sheets, presenting a two-dimensional net-like structure. Electrochemical measurement showed that the as-prepared porous NiO nanosheets delivered higher capacity than bulk NiO after 30 cycles. The good electrochemical performance of porous NiO nanosheets can be attributed to its two-dimensional net-like structure which offers good electric contact with electrolyte, short pathways for lithium ions diffusion, and good tolerance of volume change.

ACKNOWLEDGEMENTS

This work is financially supported by grants from the Key Basic Research Programs of Science and Technology Commission Foundation of Shanghai (No. 10JC1401500), Science & Technology Commission of Shanghai Municipality (No. 08DZ2270500) and the National High Technology Research and Development Program ("863" Program, No. 2009AA033701).

References

1. P Poizot, S Laruelle, S Grugeon, JM Tarason, *Nature*, 407 (2000) 496.
2. JM Tarascon, M Armand, *Nature*, 414 (2001) 359.
3. P Poizot, S Laruelle, S Grugeon, JM Tarascon, *J. Electrochem. Soc.*, 149 (2002) A1212.
4. Y Wang, QZ Qin, *J. Electrochem. Soc.*, 149 (2002) A873.
5. YM Kang, MS Song, JH Kim, HS Kim, MS Park, JY Lee, HK Liu, SX Dou, *Electrochim. Acta*, 50 (2005) 3667.
6. J Chen, L Xu, LX Gou, *Adv. Mater.*, 17 (2005) 582.
7. E Hosono, S Fujihara, I Honma, H Zhou, *Electrochem. Commun.*, 8 (2006) 284.
8. G Gachot, S Grugeon, M Armand, S Pilard, P Guenot, JM Tarascon, S Laruelle, *J. power sources*, 178 (2008) 409.
9. Q Pan, L Qin, J Liu, H Wang, *Electrochim. Acta*, 55 (2010) 5780.
10. JW Xu, CH Jia, B Cao, WF Zhang, *Electrochim. Acta*, 52 (2007) 8044.
11. LM Li, XM Yin, S Liu, YG Wang, LB Chen, TH Wang, *Electrochem. Commun.*, 12 (2010) 1383.
12. JY Jiang, J Liu, R Ding, X Ji, Y Hu, X Li, A Hu, F Wu, Z Zhu, X Huang, *J. Phys. Chem. C*, 114 (2010) 929.
13. B Varghese, MV Reddy, Z Yanwu, CS Lit, TC Hoong, GVS Rao, BVR Chowdari, ATS Wee, CT Lim, CH Sow, *Chem. Mater.*, 20 (2008) 3360.
14. S Wang, J Zhang, C Chen, *J. Power Sources*, 195 (2010) 5379.
15. L Yuan, ZP Guo, K Konstantinov, P Munroe, HK Liu, *Electrochem. Solid-State Lett.*, 9 (2006) A524.
16. X Guo, X Lu, X Fang, Y Mao, Z Wang, L Chen, X Xu, H Yang, Y Liu, *Electrochem. Commun.*, 12 (2010) 847.
17. XH Huang, JP Tu, B Zhang, CQ Zhang, Y Li, YF Yuan, HM Wu, *J. Power Sources*, 161 (2006) 541.
18. SA Needham, GX Wang, HK Liu, *J. Power Sources*, 159 (2006) 254.
19. L Liu, Y Li, SM Yuan, M Ge, MM Ren, CS Sun, Z Zhou, *J. Phys. Chem. C*, 114 (2010) 251.
20. XH Huang, JP Tu, CQ Zhang, F Zhou, *Electrochim Acta*, 55 (2010) 8981.